International Journal of Mineral Processing, 12 (1984) 55--72
Elsevier Science Publishers B.V., Amsterdam — Printed in The Netherlands

ELECTROCHEMICAL FLOTATION OF SULFIDES: REACTIONS OF CHALCOCITE IN AQUEOUS SOLUTION

G.W. WALKER, J.V. STOUT, III, and P.E. RICHARDSON

Bureau of Mines, U.S. Department of the Interior, Avondale Research Center, Avondale, MD 20782 (U.S.A.)

(Received June 16, 1982; accepted for publication March 28, 1983)

ABSTRACT

Walker, G.W., Stout, J.V., III, and Richardson, P.E., 1984. Electrochemical flotation of sulfides: reactions of chalcocite in aqueous solution. Int. J. Miner. Process. 12: 55—72.

This paper discusses the first phase of a U.S. Bureau of Mines study to use electrochemical techniques to control sulfide flotation with the aim of developing new methods to recover minerals from progressively lower grade, more complex ores. It has been established that: (1) under slow potentiodynamic sweeps or potentiostatic conditions, the current-voltage characteristics of chalcocite bed electrodes are essentially the same as those of single electrodes: (2) reactions in the chalcocite-0.05 *M* borate system can be studied quantitatively using a combination of spectrophotometric and electrochemical techniques; and (3) the reactions can be correlated with the collectorless flotation response. A microflotation-electrochemical cell, utilizing a packed bed of conducting sulfide mineral particles as the working electrode, was used to obtain correlations between the electrochemical reactions occurring on the bed and flotation response. Continuous analysis of the electrolyte by fast-scan UV spectrometry was used to monitor solution chemistry

INTRODUCTION

As early as 1931, Kamienski reported studying electrochemical reactions in sulfide flotation systems. The idea that such reactions may be important in conferring hydrophobicity was reinforced by Salamy and Nixon (1953) when they established that xanthate could be oxidized to the dixanthogen on mercury electrodes and suggested a similar reaction may produce hydrophobic disulfide layers on sulfide minerals. Additional studies in the 1950's and 1960's (Kamienski and Pomianowski, 1954; Plaksin and Bessonov, 1957; Tolun and Kitchener, 1964; Majima and Takeda, 1968; Toperi and Tolun, 1969; Yahar et al., 1969) provided further evidence that electrochemical reactions may occur in flotation systems. However, it was not until the early 1970's, largely through the pioneering studies of Australian researchers (Woods, 1971, 1972; Gardner and Woods, 1973), that electrochemical techniques were shown to be useful in controlling hydrophobicity (Woods, 1971, 1972) and flotation (Gardner and Woods, 1973; Chander and Fuerstenau, 1975) in certain mineral-collector systems.

0301-7516/84/$03.00

Thiol collectors such as the xanthates and dithiophosphates are known to form metal-collector complexes and in some cases to form sulfur-sulfur-bonded compounds such as dixanthogen. In addition, the mineral-collector interactions are observed to take place by both charge transfer and noncharge transfer reactions. However, there is not a clear understanding of either the mechanisms or kinetics involved in the interactions or the relative importance of the charge transfer and noncharge transfer reactions to the flotation process. This lack of a detailed understanding of the physical chemistry of sulfide flotation results from the complexity of the reactions that can occur between minerals and collectors in aqueous solution and from the absence of suitable in situ analytical techniques capable of measuring submonolayer quantities of absorbed species.

Although electrochemical measurements are sensitive to extremely small changes in surface coverage, they directly measure only those processes that occur via charge transfer and have usually been carried out on massive samples whose flotation response cannot be determined. One alternative is to use a bed of particles as an electrode, which should also permit taking advantage of the inherently large surface areas characteristic of particulate systems and relatively small solution volumes to continuously monitor the solution phase spectrophotometrically. Particulate bed electrodes of conducting particles were previously used by Gardner and Woods (1973) to study the ethylxanthate flotation of gold, lead, and galena, and by Chander and Fuerstenau (1975) to study the dithiophosphate flotation of chalcocite. Although the results of both studies were promising, this work was not pursued in detail, probably because once a bed floated, particle-to-particle contact was lost and no further electrochemical studies were possible. Apparently no attempts were made to utilize the enhanced analytical sensitivity possible with large-area beds to monitor the solution phase.

This paper (1) describes a microflotation-electrochemical cell in which particulate bed electrodes can be compacted for electrochemical conditioning to permit studies even when the bed is hydrophobic, (2) discusses a spectroelectrochemical study of the reactions occurring on the chalcocite bed electrodes in the absence of a collector, and (3) correlates these reactions with the natural flotation and depression of chalcocite.

This work was carried out as part of Bureau of Mines research directed towards gaining a better understanding of the physical chemistry of the flotation process with the eventual aim of developing more efficient methods of recovering minerals from complex, low-grade ores. One phase of this work, described here, includes an electrochemical study of reactions in sulfide-aqueous solution systems in the absence of a collector. As will be shown, such reactions determine the composition of both the mineral surface and the solution phase. Since collectors can react via homogeneous solution and heterogeneous surface processes, a qualitative understanding of the chemistry of both phases is a requisite for studying subsequent reactions with collectors.

EXPERIMENTAL

Figure 1 illustrates the electrochemical-microflotation cell used in these studies. A coiled platinum wire lead, entering at (F) and resting on the ground glass frit (E), served as the electrical connection to the mineral bed. A platinized platinum wire, housed in a fine porosity fritted tube (H), served as the counter electrode, and the tube itself served as a plunger to compact the particles to ensure physical and electrical contact throughout the bed. The fine porosity frit (ASTM 4 – 5.5 μm) prevented diffusion of solutions between the counter and working electrode compartments. Potentials were measured against a saturated Calomel electrode using a Luggin capillary connection through port B. Ports A and C respectively served as the inlet and outlet for electrolyte circulation.

For flotation tests, the counter electrode plunger was raised until the fritted tube was above the center tube but still making electrical contact with the electrolyte (Fig. 1). In this configuration, N_2 entering through port D was bubbled through the frit and bed, and any particles levitated by the bubbles were deflected by the counter electrode compartment and deposited around the outside of the center tube. After flotation was complete, the cell head (G) could be raised to return the particles to the bed.

A diagram of the instrumentation and flow system used in this study is shown in Fig. 2. The bed potential was controlled with a PAR 371 potentiostat and potentiodynamic i-E_a curves recorded on a Bascom-Turner 8110

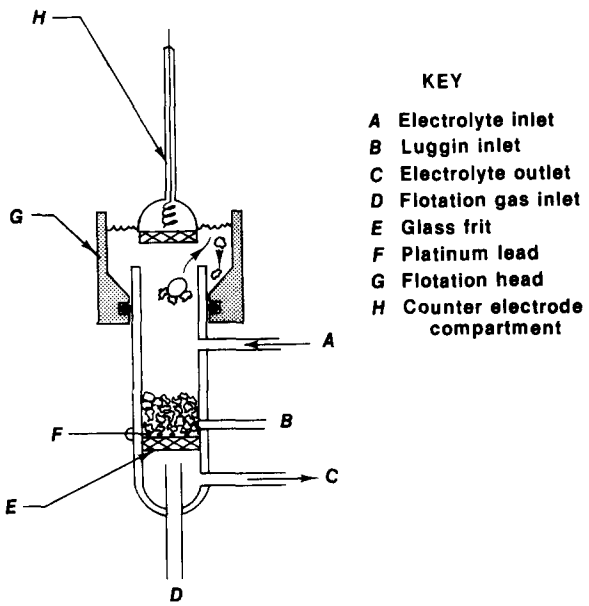

Fig. 1. Microflotation-electrochemical cell

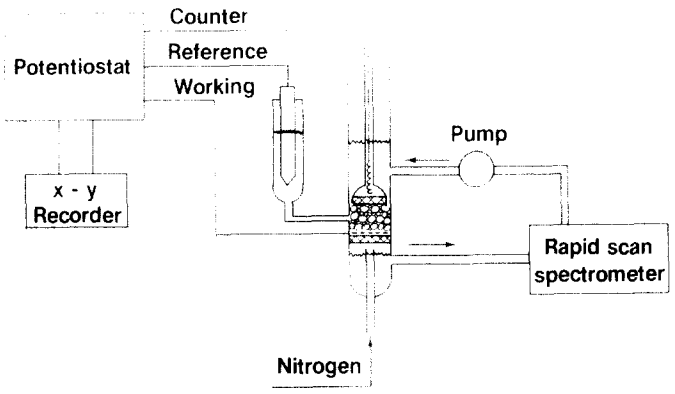

Fig. 2. Diagram of spectroelectrochemical system

digital recorder *. Electrolyte was continuously circulated between the cell and a Hewlett-Packard 8450 rapid-scan spectrophotometer. The pump element and flow tubing were Teflon to minimize extraneous contaminants. The spectrophotometer measures an entire spectrum (200 – 800 nm) in 1 sec. The 1-sec scan can either be displayed or stored and averaged with other spectra over a selected period (usually 10 sec) in order to increase resolution. At pump speeds of 60 to 70 ml/sec, any measurable chromophore produced at the bed can be detected within 2 to 4 sec, and uniform mixing of the electrolyte occurs within ≈15 sec. The total volume of electrolyte contained in the cell, tubing, cuvette, and pump was 12 to 13 ml during electrochemical testing. Using a 1.4-g sample of mineral with an approximate surface area of 0.0058 m^2/g produced a large surface area to electrolyte volume ratio, which ensured a relatively high spectrophotometric sensitivity for detection of soluble products with UV-vis chromophores.

The electrolyte used in these studies was 0.05 *M* sodium borate, which produced a naturally buffered solution of pH 9.2. The borate solution was prepared from Fisher Grade sodium tetraborate and diluted with 18 MΩ water from a Barnsted/Millipore Super Q system. Ultra-high-purity nitrogen (99.998%) was passed over hot copper turnings to eliminate trace quantities of oxygen prior to entry into the cell. Hand-selected chalcocite from Messina, Transvaal, was ground dry with a mortar and pestle, sized to 590—840 μm, washed in distilled water to remove fines, and then vacuum dried and stored in airtight containers.

RESULTS AND DISCUSSION

Electrochemical characterization of bed electrodes

The semiconducting nature of most sulfide minerals and their low solubilities in aqueous solutions have enabled these materials to be used routinely

* Reference to specific trade names does not imply endorsement by the Bureau of Mines.

as single-particle electrodes. However, in the case of bed electrodes, the cumulative effect of particle-to particle contact resistance and small electrolyte pores on the potentiodynamic response is unknown. One obvious first step in characterizing the electrochemical behavior of beds was to measure the total potential drop, ΔE, across the bed during linear voltammetry sweeps. Measurement of ΔE was achieved by monitoring the difference between the applied potential, E_a, at the bottom of the cell and a platinum screen inserted between the top of the bed and the counter electrode compartment. Pressure from the counter compartment ensured good physical contact between the particles and between the particles and the screen. Figure 3 shows a comparison of a typical 5-mV/sec i-E_a trace with a ΔE-E_a trace for a Cu_2S bed electrode. With few exceptions, changes in ΔE are seen to parallel the changes in bed current, i_b, during application of a linear potential scan to the bed, suggesting a constant effective cell resistance such that the potential drop across the bed is directly proportional to the current (ohmic behavior). In response to variations in potential scan rate, the maximum potential difference, ΔE_{max}, was found to range from $\leqslant 5$ mV at scan rates less than 1 mV/sec to 75 mV at 20 mV/sec. When the i-E trace is replotted as a function of the potential measured at the top of the bed, the resulting voltammogram (Fig. 4) is skewed in comparison to the original. The skewing is caused by anodic currents shifting the potential at the top of the bed positively, and cathodic currents shifting the potential negatively. At the higher scan rates ($\geqslant 2$ mV/sec) the skewing was significant, but below 1 mV/sec, ΔE_{max} never exceeded 5 mV and the majority of the ΔE values were less than 1 mV. Under these slow sweep conditions, the bed potential approximates that of a single-particle electrode.

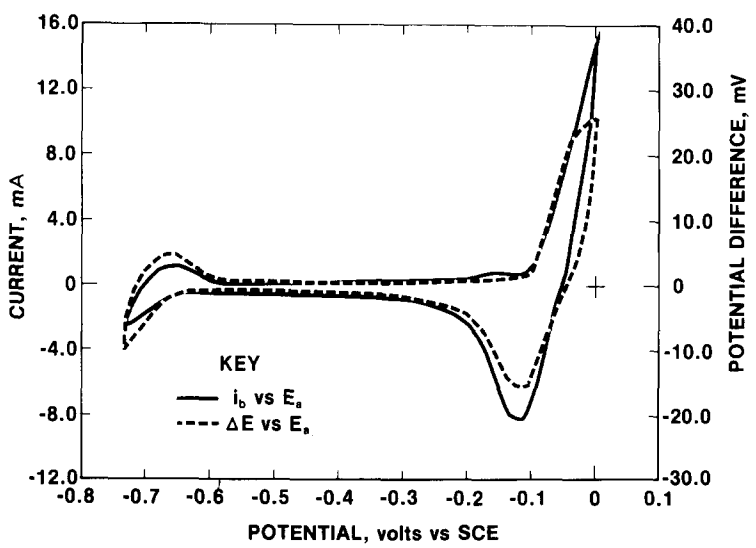

Fig. 3. Plots of bed current, i_b, and potential drop across the bed, ΔE, vs the applied potential, E_a. Sweep rate = 5mV/sec.

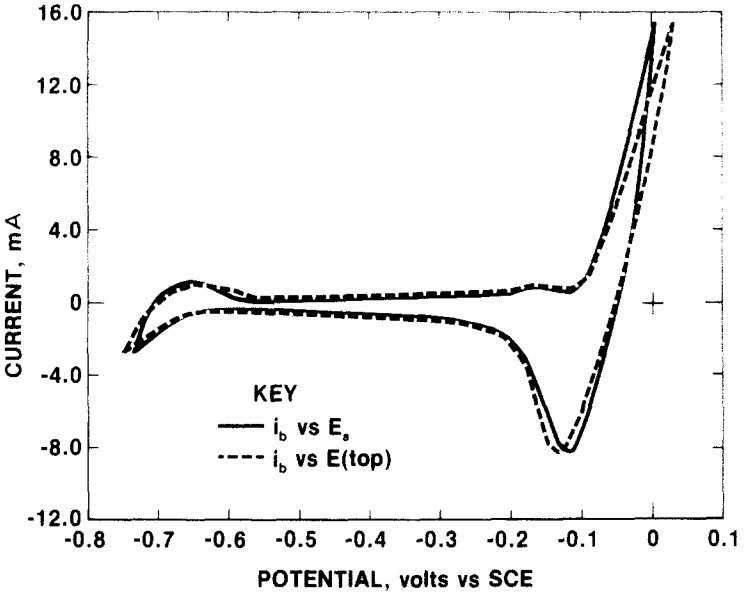

Fig. 4. Comparison between i_b-E plots using potentials measured at the top and bottom (E_a) of the Cu_2S bed. Sweep rate = 5 mV/sec.

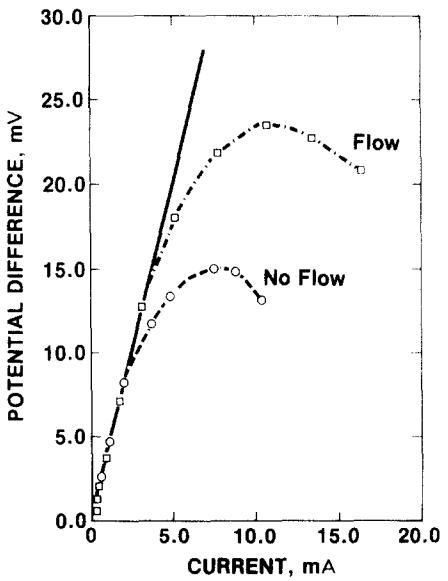

Fig. 5. Comparison of ΔE-i_b plots with and without electrolyte flow. Sweep rate = 2 mV/sec.

The major exception to the ohmic dependence of ΔE on i_b occurred at the positive limit of the applied potential. At a scan rate of 20 mV/sec (not shown), both ΔE and i_b steadily increased up the anodic limit, E_a, but at 5 mV/sec (Fig. 3), ΔE reached a plateau, and at 2 mV/sec (not shown), ΔE

peaked and then decreased, while i_b continued to increase up to the positive limit of E_a. A plot of ΔE versus i_b for corresponding values of E_a provided a convenient method for observing the dependence of ΔE on i_b. Figure 5 shows that there is an initial linear (ohmic) region, at low currents, but at higher currents ΔE deviates from a linear ohmic behavior. Circulating the solution extended the linear region and suppressed the formation of the ΔE peak observed at the slower scan rates. If the linear region represents a constant cell resistance, then the deviation of ΔE below the extrapolated linear region indicates that one of the components of the cell resistance (i.e., particle contact or electrolyte resistance within the pores) decreases at large current densities. This could be explained by the buildup of a more conducting layer at the particle contact points or by an increase in the conductivity of the electrolyte within the bed volume. The fact that circulation had such a pronounced effect on the behavior of ΔE suggests that the solution conductivity is controlling ΔE. In either case the mechanism governing changes in ΔE is complex and dynamic.

Considering the complexity of Cu_2S (to be elaborated on later), the bed voltammograms are surprisingly reproducible from one sample to another. Only small variations in fine structure, such as the anodic peak at −0.125 V in Fig. 3, generally occur. The existence of a finite ΔE might be expected to mask out fine structure, and in most instances, increasing sweep speed does decrease resolution by broadening of the peaks. However, fine-structure peaks have been seen at sweep rates >5 mV/sec. Voltammograms for single particles (Fig. 6) are basically identical to those of beds and they exhibit the same variation in fine structure from sample to sample and the same loss in resolution with increasing sweep rate. Further studies are being conducted in

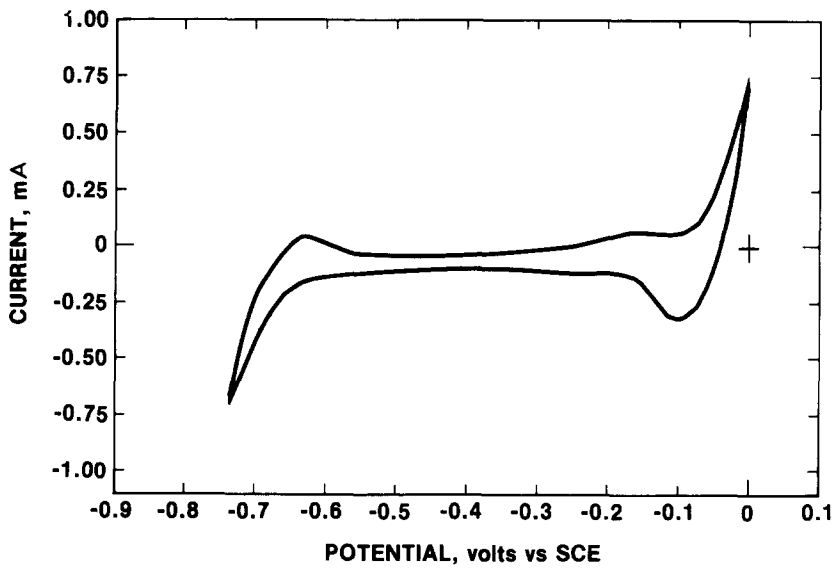

Fig. 6. Voltammogram of single particle Cu_2S electrode at a sweep rate of 5 mV/sec.

this area. However, for the purposes of the present paper, a potential drop of ≤ 1 mV observed under slow potential sweep or potentiostatic conditions is sufficient to establish that a mineral bed can operate as a single-particle electrode.

Open-circuit dissolution

Figure 7 illustrates the change in UV absorbance over a 16-min period after Cu_2S was inserted into the cell and allowed to stand in 0.05 *M* sodium borate at its open circuit potential. The absorbance bands at 216 and 294 nm were found to increase steadily throughout the 16 min, but the increase does not follow a simple kinetic rate law (i.e., for reaction order $n = 0 - 3$) based on product formation. The ratio of the two bands remained constant throughout the change. The similarity in spectra between this solution and one containing $CuCl_2$ dissolved in borate (insert) suggests that the mineral is undergoing open-circuit dissolution which produces a soluble copper species. With $K_{sp}=2\times 10^{-47}$, the dissolution of Cu_2S cannot be explained by simple dissociation, but the production of a soluble copper species is consistent with a corrosion mechanism consisting of the simultaneous reduction of dissolved O_2 and oxidation of the Cu_2S. Thermodynamic calculations show that in addition to Cu^{2+} several other soluble species, primarly $CuOH^+$, $Cu_2(OH)_2^{2+}$, $HCuO^-$, and CuO_2^{2-}, are possible at pH 9.2 (Attia, 1975) The two UV bands might therefore represent different Cu^{2+} species, but if this

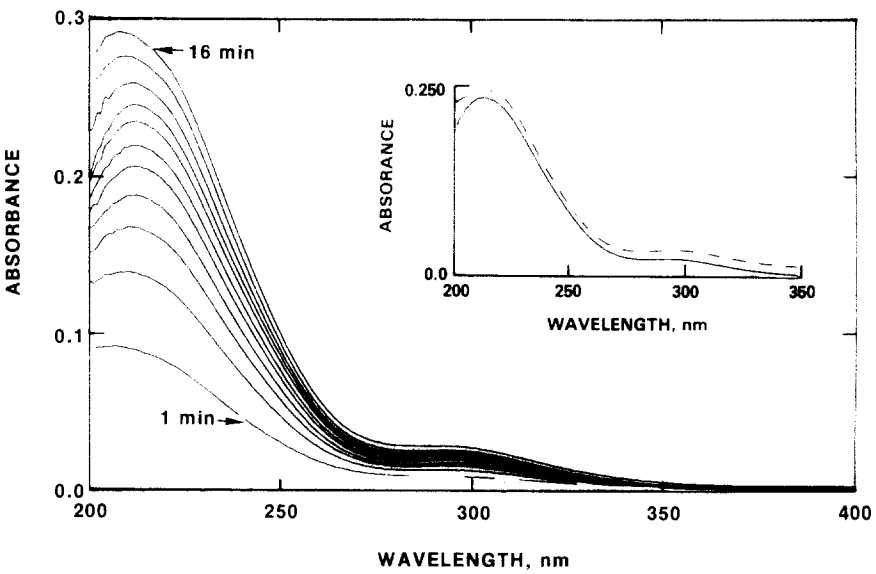

Fig. 7. UV spectrum changes of the 0.05 *M* $Na_2B_4O_7$ electrolyte during open circuit dissolution of Cu_2S. The spectra were taken every 90 sec from 1 min to 16 min. The insert compares a spectrum of the dissolution product (—) with that of $CuCl_2$ dissolved in borate solution (--); these curves are superimposable but have been offset for clarity.

is the case then the species must be in equilibrium since the ratio of the UV intensities is constant. The actual species is not known and hereafter the soluble copper species will be referred to simply as Cu(II). Given sufficient time, the soluble species should hydrolyze to insoluble $Cu(OH)_2$. However, experiments in the next section will show that for a reaction time of 7 min or less there is excellent agreement between the spectrophotometrically determined [Cu(II)] and the Cu_2S electrolysis charge. This suggests that the hydrolysis reaction is relatively slow.

Controlled potential behavior

When the open-circuit dissolution potential, E_d, is compared with a cyclic voltammogram for Cu_2S, E_d is found to coincide with the onset of the anodic current wave (O_1), This is shown in the partial i-E_a curve in Fig. 8. This figure also shows the change in UV absorbance of the solution when the applied potential was controlled above E_d. The magnitude of the absorbance bands at 216 and 294 nm were observed to steadily increase during the anodic reaction associated with the O_1 region of the insert in Fig. 8. The ratio of the two bands remained constant throughout the reaction. The spectral changes during anodic polarization are identical to the solution changes brought about by open circuit dissolution, showing that the soluble reaction products are identical in both processes. The potential scan from −0.025 to −0.1 V produced a cathodic current (R_1) and an associated decrease in the Cu(II) concentration in solution. At potentials ≤ -0.1 V, Cu(II) was no longer detectable spectrophotometrically.

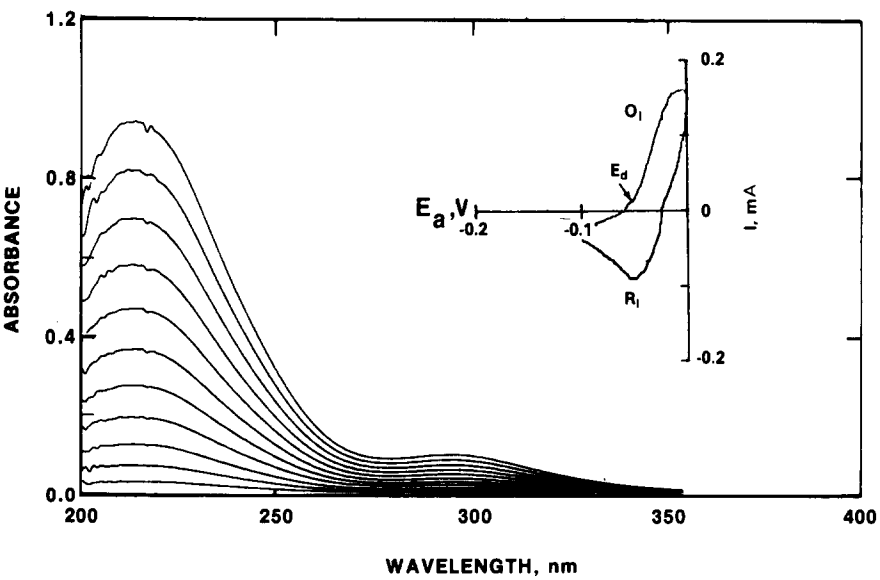

Fig. 8. UV spectrum changes of the 0.05 M $Na_2B_4O_7$ electrolyte during anodic dissolution of Cu_2S. Insert shows current associated with the O_1 reaction.

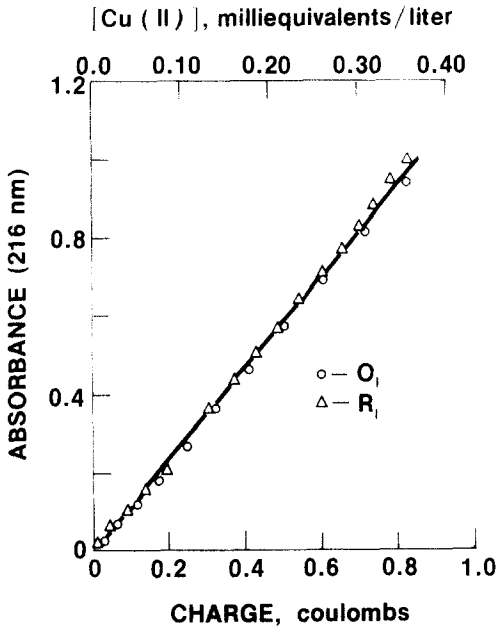

Fig. 9. Absorbance (216 nm) vs. charge for the anodic dissolution reaction (O_1) and the recombination reaction (R_1) for Cu_2S.

Figure 9 shows the relationship between the charge passed at the bed electrode and the concentration of Cu(II), as measured by the absorbance at 216 nm. The anodic charge was calculated between the potentials where the 216-nm Cu(II) band was first detected during the anodic sweep and where it began to decrease during the cathodic sweep, while the cathodic charge was measured from the point where the 216-nm band began to decrease to where it was no longer detectable. The plots are linear and virtually superimposable. Assuming an overal $2e^-$ change for the production of each Cu(II) from Cu_2S, a molar absorptivity value of 2700 l/mol-cm was obtained.

Although the spectra in Fig. 8 gave no indication of any other copper species besides those with absorbance bands at 216 and 294 nm, the tendency of Cu^{2+} to form insoluble hydroxides or oxides at a pH of 9.2 caused some concern that the total concentration of Cu(II) produced by electrolysis may not have been measured spectrophotometrically. As a means of verifying that the total Cu(II) was being measured, two alternative spectrochemical techniques were employed to measure Cu(II) in solutions containing the dissolution products of Cu_2S. One alternative consisted of a typical complexometric titration procedure employing ethylenediaminetetracetic acid (EDTA) as the titrant and monitoring the 271-nm peak of the Cu(II)-EDTA complex to find the equivalence point. In a second method, potassium ethylxanthate (KEX), a common flotation reagent, was titrated against a Cu(II) solution while monitoring the 301-nm absorption band of KEX. Comparing the Cu(II) concentrations calculated from the equivalence points

with the absorbances of the solutions prior to titration yielded molar absorptivities of ~2300 and ~2900 l/mol-cm, respectively. These values are in reasonable agreement with the value determined from electrolysis and confirm that either spectroscopic or electrolysis measurement of Cu(II) in solution is valid.

The $2e^-$/Cu(II) process in consistent with the oxidation of Cu_2S either by:

$$Cu_2S = 2Cu^{2+} + S^0 + 4e^- \quad (1)$$

or by consecutive reactions involving covellite as an intermediate:

$$Cu_2S = Cu^{2+} + CuS + 2e^- \quad (2)$$

$$CuS = Cu^{2+} + S^0 + 2e^- \quad (3)$$

Considerable controversy exists in the literature concerning the stability of S^0 in alkaline solution. There is empirical as well as thermodynamic evidence that S^0 is not stable above pH 7 (Ralston et al., 1981); however, there is sufficient experimental evidence for the existence of S^0 in alkaline solutions (Richardson and Maust, 1976; Gardner and Woods, 1979), at least in the time frame associated with cyclic voltammetry measurements ($\leqslant$10 min), to justify inclusion of S^0 as a possible reaction product.

The cathodic current leading to a decrease in Cu(II) in solution is assumed to be the reverse of the oxidation process. The equivalence in charge during the anodic and cathodic scans (Fig. 9) establishes that there is mass balance between the forward and reverse processes. Studies of Cu_2S and $CuFeS_2$ in acid solution (Koch and McIntyre, 1976; Warren, 1978), encompassing thermodynamic calculations, open-circuit potential measurements, and polarization studies, have concluded that the transition from Cu_2S to CuS proceeds through a series of stable Cu-S species represented by:

$$Cu_2S \rightarrow Cu_{1.93}S \rightarrow Cu_{1.83}S \rightarrow Cu_{1.67}S \rightarrow Cu_{1.38}S \rightarrow CuS \quad (4)$$

Studies of other sulfides, particularly PbS (Richardson and Maust, 1976; Gardner and Woods, 1979) at different pH values concluded that the dissolution reaction could occur by a variety of reactions producing metal oxides and oxygenated sulfur species such as $S_2O_3^{2-}$ and SO_4^{2-} as well as the metal ion and elemental sulfur. The predominance of one mechanism over another was reported to be dependent on the number of potential cycles as well as the potential limits of the cycle. While our proposed dissolution reaction would appear to be overly simplistic in comparison, we have not been able to observe any direct evidence supporting another mechanism. The mass balance between reactants and products would seem to be less likely when two soluble species rather than one soluble and one stationary surface species are considered, but if in fact a species such as $S_2O_3^{2-}$ was produced through a reaction of the type:

$$2Cu_2S + 6OH^- = 4Cu^{2+} + S_2O_3^{2-} + 3H_2O + 12e^- \quad (5)$$

then not only must the reverse reaction be possible but, as will be discussed later, the reduction of $S_2O_3^{2-}$ to HS^- must also be possible.

Potential scans between −0.1 and −0.5 V produced small currents (Fig. 6) which might be associated with compositional changes in the Cu_2S. There were no changes in absorbance in this potential range that could be correlated with the *i-E* curves. However, between −0.55 and −0.69 V (Fig. 10), there is a substantial cathodic current (insert) which introduces a soluble species into solution with an absorbance band at 229 nm. The magnitude of the 229 nm band increases with decreasing potential. The electrode is believed to undergo reduction in this potential region via the reaction:

$$Cu_2S + H_2O + 2e^- = 2Cu^0 + HS^- + OH^-, \qquad E_h^0 = -0.926 \tag{6}$$

or if the surface has been partially converted to CuS by prior anodic sweeping (reaction 2) then via reactions:

$$CuS + H_2O + 2e^- = Cu^0 + HS^- + OH^-, \qquad E_h^0 = -0.733 \text{ V} \tag{7}$$

or

$$2CuS + H_2O + 2e^- = Cu_2S + HS^- + OH^-, \qquad E_h^0 = -0.540 \text{ V} \tag{8}$$

Hydrosulfide (HS^-) was the likely candidate for the 229-nm band and this was confirmed when Na_2S dissolved in 0.05 M borate produced an identical UV spectrum. The appreance of an anodic current peak at −0.59 V during

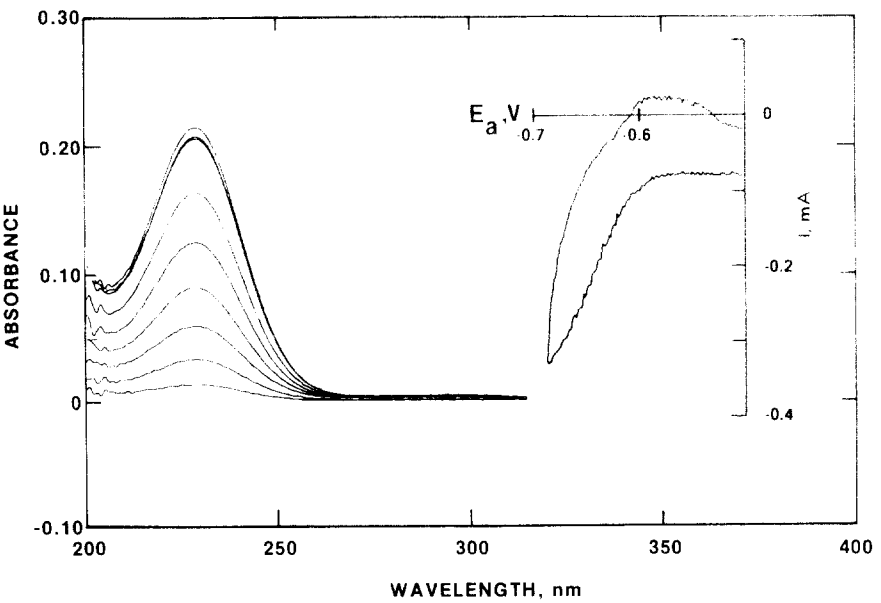

Fig. 10. Increase in absorbance during cathodic dissolution of Cu_2S between −0.55 and −0.69 V in 0.05 *M* $Na_2B_4O_7$. Insert shows the corresponding cathodic current for a potential sweep of 5 mV/sec.

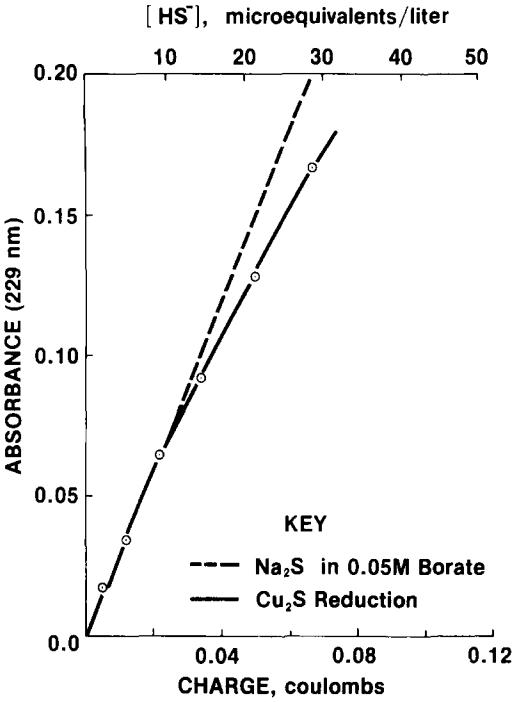

Fig. 11. Absorbance (229 nm) vs. charge for the cathodic dissolution of Cu_2S. Comparison with a Beer's law plot of HS^- in 0.05 *M* $Na_2B_4O_7$.

the positive potential scan suggested that Cu_2S or CuS was being reformed by the reverse of reactions 6, 7 or 8 and spectroscopic studies established that the 229-nm band disappeared during this portion of the anodic scan.

In contrast to the behaviour of Cu(II) illustrated in Fig. 9, Fig. 11 shows that the plot of electrolysis charge versus absorbance at 229-nm exhibits linearity only in the initial stage of HS^- production. Below approximately −0.65 V, corresponding to approximately 0.02 coulombs in Fig. 11, the plot deviates from its colinearity with a Beer's law plot of HS^-, and the deviation continues with increasing charge. There are a number of possible explanations for this deviation, including consumption of HS^- in a parallel reaction or competition between HS^- formation and another surface reaction. However, further studies established that in aqueous solutions at pH 9.2: (1) HS^- disappeared from capped and uncapped solutions; (2) its disappearance was accelerated by nitrogen and oxygen bubbling; (3) addition of a reactive substance such as H_2O_2 had no effect on the rate; and (4) there was a smell of "sulfide" above a stirred solution of HS^-. These results suggest that the equilibrium between HS^- and H_2S and the subsequent evaporation of H_2S from solution are the controlling forces in the decay. Even though HS^- is favored thermodynamically over H_2S in basic solution, the evaporation rate of H_2S must be sufficiently rapid and the equilibrium reestablished sufficiently fast to cause an appreciable decrease in HS^- even while it is being generated electrochemically.

An alternative mechanism for production of HS^- is by reduction of elemental sulfur:

$$S^0 + H_2O + 2e^- = HS^- + OH^- \quad (9)$$

which, from thermodynamic calculations, is predicted to occur in the region of −0.32 V. The absence of any spectrophotometrically detectable HS^- and any accompanying cathodic current in this region on the *i-E* curves could be explained by a combination of factors. Not only does the recombination of Cu_2S precede the formation of HS^- by almost 300 mV, but the depletion of S^0 by the reverse of reaction 3 is so complete that there isn't any S^0 left to produce HS^-. When an experiment was designed so that the Cu(II) dissolution product from a Cu_2S bed was replaced by flushing with pure borate, an absorbance band at 229-nm and an accompanying increase in cathodic current were observed near −0.30 V while the normal cathodic current peak between −0.025 and −0.09 V was absent. At −0.60 V, during the same potential sweep, the 229-nm adsorbance band and a cathodic current appeared with magnitudes equivalent to those observed under normal conditions. Therefore, hydrosulfide ion can be formed by reactions 6—9, but unless the Cu(II) is physically removed from solution, reaction 3 depletes the surface sulfur so that reaction 9 is not observed.

Referring back to the discussion on the possible production of an oxygenated sulfur species (i.e., $S_2O_3^{2-}$) during anodic dissolution, the above experiment suggests that oxysulfur ions are not major reaction products. Assuming that $S_2O_3^{2-}$ were present and could be electrochemically reduced to form HS^-, the soluble $S_2O_3^{2-}$ in the preceding experiment would have been removed from the cell during the change of electrolyte. Under these circumstances, HS^- would only have been observed at −0.62 V.

Natural flotation

Having obtained a general understanding of the electrochemical behavior of Cu_2S in aqueous solution, the flotation of Cu_2S after electrochemical pretreatment was studied to correlate the surface reactions with natural hydrophobicity.

In all experiments involving flotation, the Cu_2S was introduced into a 0.05 *M* borate solution and allowed to equilibrate at open circuit (≃ 10 min) while the solution was purged of dissolved O_2. The buildup of Cu(II) in solution was monitored spectroscopically during this period. Flotation is expressed as the percent of the bed that floated in 2 min using N_2 as the carrier gas. Recovery was visually estimated from the height of the mineral bed. Measurements of this type gave exact readings for zero and 100% recovery; between these extremes, accuracy was estimated to be ±10% of the stated recovery values.

To determine the effect of electrochemical potential on flotation response, the bed was compacted and potentiostatically controlled at the de-

sired potential for 10 min immediately prior to the 2-min float tests. At the end of each flotation test, the floated fraction was returned to the float chamber, recompacted, and potentiostated at a new potential.

Figures 12 and 13 illustrate the results of two separate studies of the effect of electrochemical pretreatment on the flotation response using supposedly identical beds of Cu_2S. Although the exact magnitudes of recovery versus potential curves for these two tests differ considerably, the general dependence of flotation on potential is nearly the same. In additional studies using Cu_2S from the same source, the recovery curves exhibited similar features but with the recoveries falling between the limits of those in Figs. 12 and 13.

For all the Cu_2S bed studies, the recovery after conditioning on open circuit for 10 min was zero. Subsequent conditioning at negative potentials (curve 1 in both Figs.) produced an increase in flotation with a maximum recovery of $\simeq 20\%$ near -0.4 V followed by a decrease to zero at -0.6 V. Continued conditioning at progressively increasing potentials from -0.6 to 0.0 V produced an increase in recovery, reaching $\simeq 90\%$ at 0 V in one test (curve 2, Fig. 12) and $\simeq 60\%$ at -0.1 V in another test (curve 2, Fig. 13). Above 0 V, recovery drops sharply, reaching zero at 0.2 V (curve 2, Fig. 12). When the potential was stepped back into the cathodic region (curve 3, Fig. 12), recovery again increased and its magnitude was usually in between the preceding cathodic and anodic sequences. In Fig. 13 the anodic potential sequence (curve 2) was stopped at -0.10 V and then stepped cathodically

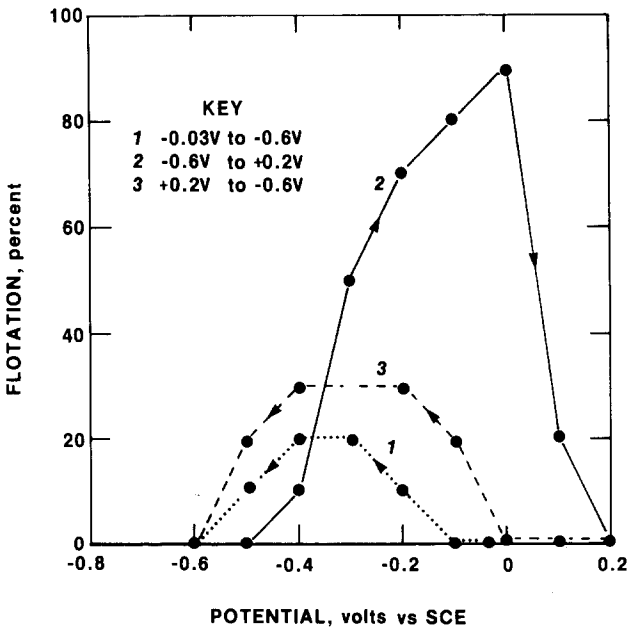

Fig. 12. Flotation recovery vs. applied potential for chalcocite in 0.05 M $Na_2B_4O_7$.

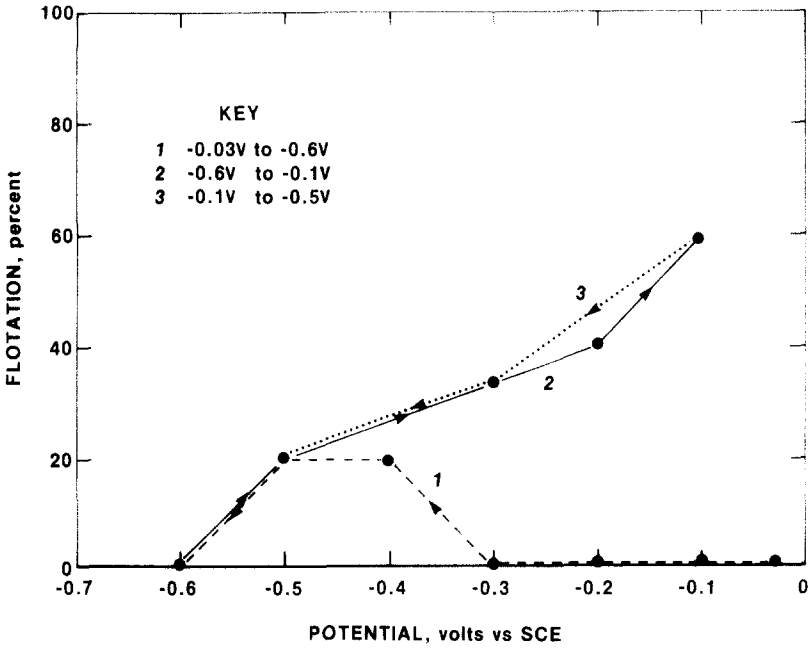

Fig. 13. Flotation recovery vs. applied potential for chalcocite in 0.05 *M* $Na_2B_4O_7$.

(curve 3). Under these conditions, the magnitudes of the anodic and cathodic recovery curves were virtually identical. When the bed potential was lowered to −0.70 V (not shown), the ability to return the mineral to a hydrophobic state was irreversibly lost.

Comparing the potential dependent flotation response to a voltammogram of Cu_2S, (Fig. 3) one can make some qualitative correlations:

(1) The inability of Cu_2S to float at its open circuit potential can be attributed to the presence of hydrophilic oxides or hydroxides which formed by exposure to air or during the initial equilibration stage in the borate solution. Although Cu(II) has been identified as an open circuit dissolution product and reaction 1 implies the presence of elemental sulfur, a highly hydrophobic substance, its concentration is apparently not sufficient to promote collectorless flotation. In this regard, it should be noted that the initial stages of anodic dissolution are not expected to produce elemental sulfur but rather to alter the stoichiometry of the surface in the sulfur-rich direction, with sulfur nucleation occurring only after its concentration exceeds its solubility in the mineral.

(2) The slight increase in flotation at moderate reducing potentials may arise from two separate processes: (a) the reduction of hydrophilic oxide or hydroxide groups; and (b) the simultaneous reformation of Cu_2S (or other Cu-S compounds) on the surface via a reaction with the Cu(II) dissolution product produced by open circuit dissolution.

(3) The decrease in recovery at −0.6 V corresponds to the onset of the

cathodic dissolution wave on the cyclic voltammetry curve and the simultaneous appearance of HS^- in solution (Fig. 10). Again, the onset of the cathodic dissolution wave may not necessarily correspond to the two-phase system of Cu_2S and Cu^0 resulting from reaction 6, but may represent reactions whereby the host lattice is enriched in copper. The subsequent formation of copper hydroxide on the copper-enriched surface may account for the decrease in flotation. Interestingly, stronger reducing conditions (-0.7 V) produce irreversible loss of floatability. The irreversible loss of floatability may result because a portion of the soluble sulfur (reaction 6(is lost by evaporation of H_2S, preventing the complete conversion of Cu^0 back to Cu_2S at the higher potentials. Under these conditions the remaining Cu^0 can react to form oxides or hydroxides which render the surface hydrophilic.

(4) Maximum natural flotation occurs between -0.03 and 0.0 V. This is probably a result of either elemental sulfur or excess sulfur in the lattice such that the coordination of surface copper with sulfur is at a maximum, inhibiting hydroxide formation.

(5) We have not yet studied the electrochemistry of Cu_2S above 0 V. However, the sudden dropoff in flotation may represent oxidation reactions leading to $S_2O_3^{2-}$ or other soluble sulfur products and copper hydroxides.

CONCLUSIONS

Measurement of the potential difference across a bed of Cu_2S has established that, under a fairly wide range of conditions, a uniform potential exists throughout the bed. With this criterion established, the electrochemical reactions of Cu_2S in a borate solution and the resulting changes in the solution composition were investigated. At open circuit, Cu_2S undergoes anodic dissolution with the resulting buildup of a soluble copper species and an oxidized sulfur species. By controlling the potential to values anodic to the open circuit potential, the production of soluble copper is accelerated and the concentration of Cu(II) as measured by its 216-nm band is directly proportional to the quantity of charge passed. The reverse of this reaction, which causes a decrease in the Cu(II) absorption band, follows the identical relationship between charge and [Cu(II)]. At -0.60 V a cathodic reaction is observed that results in the buildup of HS^- in solution. Plots of charge vs HS^- absorbance (229-nm) are nonlinear because of the loss of HS^- through its equilibrium with H_2S and subsequent evaporation from solution. Comparison between collectorless flotation and electrochemical behavior has shown that as long as the applied potential is maintained within the limits of electroinactivity (-0.10 to -0.50), varying degrees of flotation are possible. Anodic potential above 0 V caused a rapid decrease in flotation, which could be restored by subsequent polarization between -0.1 and -0.5 V. However, potentials below -0.6 V caused an irreversible loss in flotation.

REFERENCES

Attia, Y.A., 1975. Surface chemistry of copper minerals in water. Trans. Inst. Min. Metall., 85: C221–230.

Chander, S. and Fuerstenau, D.W., 1975. On the floatability of sulfide minerals with thiol collectors: the chalcocite-diethyldithiophosphate system. In: Proceedings of the XIth Int. Min. Proc. Cong., Rome, pp. 583–604.

Gardner, J.R. and Woods, R., 1973. The use of particulate bed electrodes for the electrochemical investigation of metal and sulfide flotation. Aust. J. Chem., 26: 1635–1644.

Gardner, J.R. and Woods, R., 1979. A study of the surface oxidation of galena using cyclic voltammetry. J. Electroanal. Chem., 100: 447–459.

Kamienski, B., 1931. So-called flotation. Przem. Chem., 15: 201–202.

Kamienski, B. and Pomianowski, A., 1954. The influence of hydrogen ion on the potential of a mineral electrode during the process of flotation. Bull. Acad. Polon. Sci., C1 III, 2: 85–89.

Koch, D.F.A. and McIntyre, R.J., 1976. The application of reflectance spectroscopy to the study of anodic oxidation of cuprous sulfide. J. Electroanal. Chem., 71: 285–296.

Majima, H. and Takeda, M., 1968. Electrochemical studies of the xanthate-dixanthogen system on pyrite. Trans. Soc. Min. Eng., AIME, 241: 431–436.

Plaksin, I.N. and Bessonov, S.V., 1957. Role of gases in flotation reactions. IInd Int. Cong. of Surface Activity. Butterworth, London, III: 361–367.

Ralston, J., Alabaster, P. and Healy, T.W., 1981. Activation of zinc sulphide with Cu(II), Cd(II) and Pb(II): III. The mass-spectrometric determination of elemental sulphur. Int. J. Miner. Process., 7: 175–201.

Richardson, P.E. and Maust, E.E., Jr., 1976. Surface stoichiometry of galena in aqueous electrolytes and its effect on xanthate interactions. In: M.C. Fuerstenau (Editor), Flotation: A.M. Gaudin Memorial Volume 1. AIME, New York, pp. 364–392.

Salamy, S.G. and Nixon, J.C., 1953. The application of electrochemical methods to flotation research. In: Recent Developments in Mineral Dressing. IMM, London , pp. 503–516.

Tolun, R. and Kitchener, J.A., 1964. Electrochemical study of the galena-xanthate-oxygen flotation system. Trans. IMM, 73: 312–322.

Toperi, D. and Tolun, R., 1969. Electrochemical study and thermodynamic equilibria of the galena-oxygen-xanthate flotation system. Trans. IMM, 78: 191–197.

Warren, G.W., 1978. The electrochemical oxidation of $CuFeS_2$. Ph.D. Dissertation, Univ. of Utah.

Woods, R., 1971. The oxidation of ethylxanthate on platinum, gold, copper, and galena electrodes, Reltationship to the mechanism of mineral flotation. J. Phys. Chem., 75: 354–362.

Woods, R., 1972. The anodic oxidation of ethylxanthate on metal and galena electrodes. Aust. J. Chem., 25: 2329–2335.

Yahar, B., Haydon, B.C. and Kitchener, J.A., 1969. Electrochemistry of the galena-diethyldithiocarbamate-oxygen flotation system. Trans. IMM, 78: 181–184.